# Low Energy Spin Waves and Magnetic Interactions in SrFe$_2$As$_2$

Jun Zhao,[1] Dao-Xin Yao,[2] Shiliang Li,[1] Tao Hong,[3] Y. Chen,[4] S. Chang,[4] W. Ratcliff II,[4] J. W. Lynn,[4] H. A. Mook,[3]
G. F. Chen,[5] J. L. Luo,[5] N. L. Wang,[5] E. W. Carlson,[2] Jiangping Hu,[2] and Pengcheng Dai[1,3,]*

[1]*Department of Physics and Astronomy, The University of Tennessee, Knoxville, Tennessee 37996-1200, USA*
[2]*Department of Physics, Purdue University, West Lafayette, Indiana 47907, USA*
[3]*Neutron Scattering Science Division, Oak Ridge National Laboratory, Oak Ridge, Tennessee 37831-6393, USA*
[4]*NIST Center for Neutron Research, National Institute of Standards and Technology, Gaithersburg, Maryland 20899-6102, USA*
[5]*Institute of Physics, Chinese Academy of Sciences, P.O. Box 603, Beijing 100190, China*
(Received 18 August 2008; published 14 October 2008)

We report inelastic neutron scattering studies of magnetic excitations in antiferromagnetically ordered
SrFe$_2$As$_2$ ($T_N$ = 200–220 K), the parent compound of the FeAs-based superconductors. At low tem-
peratures ($T$ = 7 K), the magnetic spectrum $S(Q, \hbar\omega)$ consists of a Bragg peak at the elastic position
($\hbar\omega = 0$ meV), a spin gap ($\Delta \leq 6.5$ meV), and sharp spin-wave excitations at higher energies. Based on
the observed dispersion relation, we estimate the effective magnetic exchange coupling using a
Heisenberg model. On warming across $T_N$, the low-temperature spin gap rapidly closes, with weak
critical scattering and spin-spin correlations in the paramagnetic state. The antiferromagnetic order in
SrFe$_2$As$_2$ is therefore consistent with a first order phase transition, similar to the structural lattice
distortion.

The parent compounds of the high-transition tempera-
ture (high-$T_c$) copper oxides are simple antiferromagnetic
(AF) Mott insulators [1] characterized by a very strong
nearest neighbor AF exchange coupling $J$ ($>100$ meV) in
the CuO$_2$ planes [2]. When holes or electrons are doped
into the CuO$_2$ planes, the character of the ground state is
fundamentally altered from an AF insulator to a supercon-
ductor with persistent short-range AF spin correlations
(excitations) [3]. In the case of FeAs-based superconduc-
tors such as $R$FeAsO$_{1-x}$F$_x$ (where $R$ = La, Nd, Sm, Pr,...)
[4–7] and $A_{1-x}B_x$Fe$_2$As$_2$ ($A$ = Ba, Sr, Ca, $B$ = K, Cs, Na)
[8–11], although the undoped parent compounds are also
long-range ordered antiferromagnets with a collinear spin
structure as shown in Fig. 1(a) [12–16], much is unknown
about the magnetic exchange coupling responsible for such
a spin structure. For example, early theoretical studies
suggested that LaFeAsO has a spin-density-wave (SDW)
instability [17,18]. As a consequence, the AF spin structure
in these materials arises from quasiparticle excitations
across electron-hole pockets in a nested Fermi surface
[19], much like SDW antiferromagnetism in metallic chro-
mium (Cr) [20]. Alternatively, a Heisenberg magnetic
exchange model [21–24] is suggested to explain the AF
structure. Here, the collinear spin phase is stable when the
nearest neighbor exchange $J_1$ and the next nearest neighbor
exchange $J_2$ satisfy $J_1 < 2J_2$ [Fig. 1(a)]. First-principles
calculations estimate $J_1 \sim J_2$ [23]. In contrast, some band
structure calculations [25] suggest that the $J_1$ along the $a$
axis and $b$ axis of the low-temperature orthorhombic struc-
ture ($c > a > b$) can have different signs with $J_{1a}$ and $J_{1b}$
being AF and ferromagnetic, respectively, and that $J_{1a} >
2J_2$. Therefore, there is no theoretical consensus on the

relative strengths of $J_{1a}$, $J_{1b}$, and $J_2$ or the microscopic
origin of the observed AF spin structure. If magnetism is
important for superconductivity of these materials, it is
essential to establish the "effective Hamiltonian" that
can determine the magnetic exchange coupling.

In this Letter, we report inelastic neutron scattering
studies of spin-wave excitations in single crystals of
SrFe$_2$As$_2$ [15,26,27]. At low temperature, we find that
spin waves have an anisotropy gap of $\Delta = 6.5$ meV and
disperse rapidly along both the [$H$, 0, 0] and [0, 0, $L$] direc-
tions. On warming to 160 K, the magnitude of the spin gap
decreases to 3.5 meV while the intensities of the spin-wave
excitations follow the expected Bose statistics. However,
there are only weak critical scattering and magnetic corre-
lations in the paramagnetic state at 240 K, in sharp contrast
to the SDW excitations in Cr [20] and spin waves in
cuprates [2,3]. We estimate the effective magnetic ex-
change coupling using a Heisenberg model and find that
$J_{1a} + 2J_2 = 100 \pm 20$ meV, $J_z = 5 \pm 1$ meV, with a mag-
netic single ion anisotropy $J_s = 0.015 \pm 0.005$ meV. The
weak critical scattering and paramagnetic spin-spin corre-
lations, together with the simultaneous first order structural
transition [15], suggest a first order AF phase transition.

Our experiments were carried out on HB-1 triple-axis
spectrometer at the High Flux Isotope Reactor, Oak Ridge
National Laboratory, and BT-7 and SPINS triple-axis spec-
trometers at the NIST Center for Neutron Research. For
HB-1 and BT-7 measurements, we fixed the final neutron
energy at $E_f$ = 14.7 meV and used PG(0,0,2) (pyrolytic
graphite) as monochromator and analyzer. A PG filter was
placed in the exit beam path to eliminate $\lambda/2$. For the
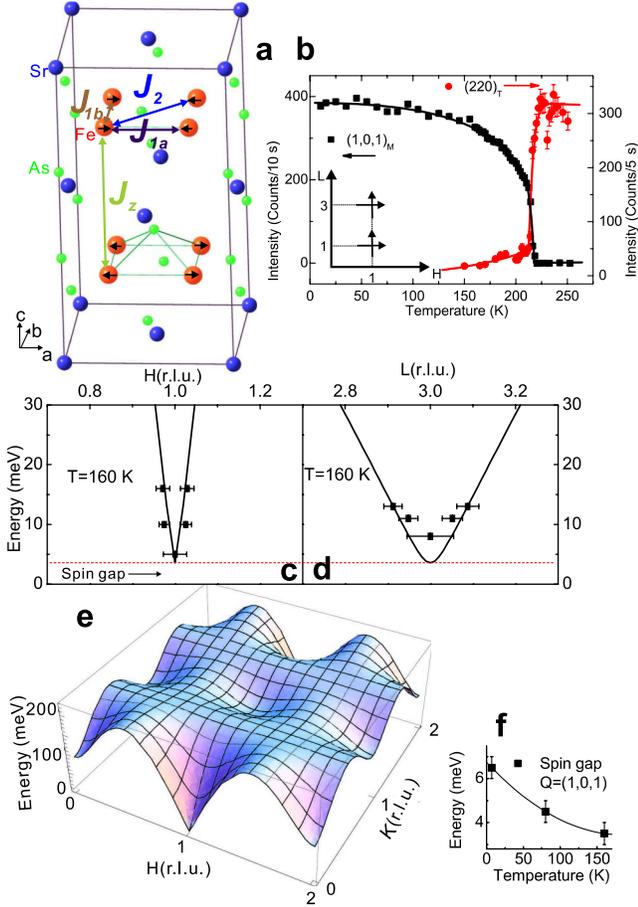SPINS measurements, the final neutron energy was fixed at

FIG. 1 (color online).    (a) The Fe spin ordering in the SrFe$_2$As$_2$ chemical unit cell and magnetic exchange couplings along different high-symmetry directions. (b) The AF Néel temperature and the temperature dependence of the structural (2, 2, 0) Bragg peak for one of the SrFe$_2$Sr$_2$ crystals used in the experiment [15]. The inset shows positions in reciprocal space probed in the experiment. (c) Observed spin-wave dispersion along the [H, 0, 0] direction at 160 K. (d) Similar dispersion along the [0, 0, L] direction. (e) Calculated three-dimensional spin-wave dispersions using $J_{1a} = 20$, $J_{1b} = 10$, $J_2 = 40$, $J_z = 5$, and $J_s = 0.015$ meV. (f) Temperature dependence of the anisotropy spin gap $\Delta(T)$.

$E_f = 5$ meV and a cold Be filter was placed in the scattered beam path. SrFe$_2$As$_2$ single crystals with a $T_N$ distribution from 200 to 220 K were grown from self flux [15,27] and coaligned within 2 deg to have a total mass of $\sim 0.7$ g. From earlier diffraction work [15], we know that the AF order occurs in close proximity to the lattice distortion, changing the crystal structural symmetry from tetragonal above $T_N$ to orthorhombic below it [Fig. 1(b)]. However, it is unclear whether the structural and magnetic phase transitions are second [28] or first order [29]. For the observed spin structure [Fig. 1(a)], magnetic Bragg peaks are allowed at [H, 0, L] (H, L are odd integers) reciprocal lattice units (r.l.u.), where the momentum transfer is $Q$(in Å$^{-1}$) $= (H2\pi/a, K2\pi/b, L2\pi/c)$ and $a = 5.5695(9)$, $b = 5.512(1)$, $c = 12.298(1)$ Å are lattice parameters in

the orthorhombic state at 150 K. To probe spin-wave excitations, we aligned our single crystal array in the [H, 0, L] zone, where we can probe excitations along the [H, 0, 0] and [0, 0, L] directions.

Figures 2(a) and 2(e) show constant-energy scans for $\hbar\omega = 1$ and 5 meV around [H, 0, 1] at 160 K obtained on SPINS. While the scattering at $\hbar\omega = 1$ meV is featureless [Fig. 2(a)], there is a clear peak centered at $H = 1$ in the 5 meV data [Fig. 2(e)]. This immediately suggests that spin waves in SrFe$_2$As$_2$ have an anisotropy gap at this temperature that is less than 5 meV. Moving on to higher energies, Figs. 2(b)–2(d) and 2(f)–2(h) summarize $Q$ scans along the [H, 0, 0] and [0, 0, L] directions, respectively, at different energies. The $Q$ widths of the scattering clearly become broader with increasing energy. Figures 1(c) and 1(d) show the observed dispersion curves for the limited energy range with observable spin-wave excitations. Assuming an effective Heisenberg Hamiltonian [24,30] $H = J_{1a}\sum_{i,j}\mathbf{S}_i \cdot \mathbf{S}_j + J_{1b}\sum_{i,j}\mathbf{S}_i \cdot \mathbf{S}_j + J_2\sum_{i,j}\mathbf{S}_i \cdot \mathbf{S}_j + J_z\mathbf{S}_i \cdot \mathbf{S}_j - J_s(S_i^z)^2$, where $J_{1a}$, $J_{1b}$, $J_2$, and $J_z$ are exchange interactions shown in Fig. 1(a), $J_s$ is the single ion anisotropy, and $S$ is the magnitude of iron spin, the spin-wave dispersions along the [H, 0, 0] and [0, 0, L] directions near the (1, 0, 1) Bragg peak are $E(k_x) = 2S[(J_{1a} + 2J_2 + J_s + J_z)^2 - (J_z - (J_{1a} + 2J_2)\cos k_x)^2]^{1/2}$ and $E(k_z) = 2S[(2J_{1a} + 4J_2 + J_s + J_z - J_z\cos k_z)(J_s + J_z + J_z\cos k_z)]^{1/2}$, respectively. In addition, the size of the spin gap due to the single ion anisotropy is $\Delta(1,0,1) = 2S[J_s(2J_{1a} + 4J_2 + J_s + 2J_z)]^{1/2}$. The solid lines in Figs. 1(c) and 1(d) are the best fits with
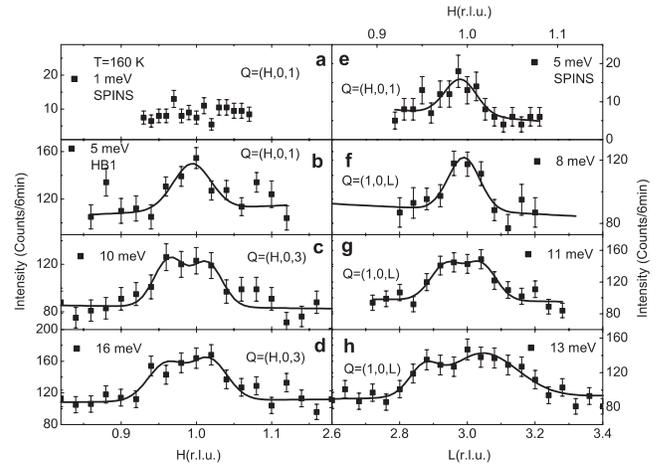


FIG. 2.    Wave vector dependence of the spin-wave excitations at 160 K obtained on cold [(a) and (e)] and thermal [(b)–(d) and (f)–(h)] triple-axis spectrometers at different energies. (a) $Q$ scan along the [H, 0, 1] direction at $\hbar\omega = 1$ meV using SPINS. The spectrum is featureless indicating the presence of a spin gap exceeding 1 meV. Identical scan at $\hbar\omega = 5$ meV in (e) shows clear evidence of spin-wave excitations centered at (1, 0, 1). (b–d) $Q$ scans along the [H, 0, 1] or [H, 0, 3] directions at different energies. The spectra clearly broaden with increasing energy. (f–h) Similar scans along the [1, 0, L] direction, which probe the exchange coupling $J_z$.

these equations, where $J_{1a} + 2J_2 = 100 \pm 20$ meV, $J_z = 5 \pm 1$ meV, and $J_s = 0.015 \pm 0.005$ meV. The three-dimensional plot in Fig. 1(e) shows the expected spin-wave dispersion at higher energies.

To determine the temperature dependence of the spin gap, we carried out energy scans at the signal and background positions for spin waves at different temperatures. At 7 K, an energy scan at the magnetic zone center position $Q = (1, 0, 1)$ shows an abrupt increase above 6.5 meV, while the background scattering at $Q = (1.2, 0, 1)$ is featureless [Fig. 3(a)]. Energy scans at equivalent positions $Q = (1, 0, 3)$ and $(0.8, 0, 3)$ in Fig. 3(b) show similar results and therefore reveal a low-temperature spin gap of $\Delta = 6.5$ meV. On warming to 80 K, identical scans at $Q = (1, 0, 1)$ and $Q = (1.2, 0, 1)$ show that the spin gap is now at $\Delta = 4.5$ meV [Fig. 3(c)]. Finally, $\Delta$ becomes 3.5 meV at 160 K, consistent with constant-energy scans in Figs. 2(a) and 2(e). These results indicate that the spin anisotropy of the system reduces with increasing temperature.

Figure 4 summarizes the temperature dependence of the spin waves and quasielastic scattering in the AF ordered and paramagnetic states obtained on SPINS and BT-7. Figure 4(a) shows energy scans at $Q = (1, 0, 1)$ for $T = 130, 160, 200, 240,$ and 280 K plotted on a log scale. When the temperature is increased across $T_N$ ($\sim 210$ K), there is a rapid decrease in the ordered moment but little evidence for quasielastic and critical scattering, which are signatures of a second order phase transition. To illustrate this point, we plot in Fig. 4(b) the temperature difference scattering using 280 K data as background. Besides the magnetic Bragg peak below $T_N$ at $\hbar\omega = 0$ meV, there is little quasielastic critical scattering typical of a second order phase transition. Figure 4(c) shows constant-energy scans ($\hbar\omega = 1$ meV) measured on SPINS, and the scattering is essentially featureless at all temperatures investigated. Assuming no spin correlations in the paramagnetic state at 280 K, the differences in the scattering between 240 and 280 K at
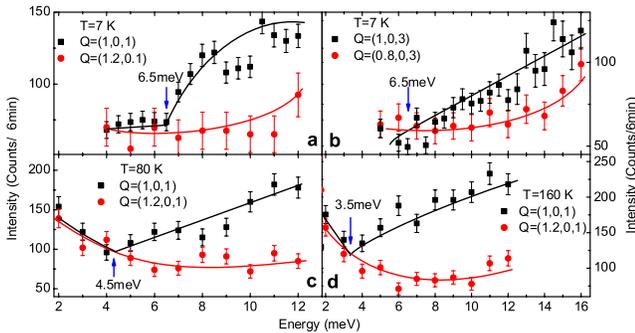
$\hbar\omega = 1$ meV should reveal the magnetic intensity gain close to $T_N$. Consistent with the temperature dependence of the energy scans in Figs. 4(a) and 4(b), there are signs of possible uncorrelated paramagnetic scattering (since the subtracted data in Fig. 4(e) are overall positive) at 240 K but weak critical scattering. For temperatures below $T_N$, we find that spin-wave excitations at temperatures below 160 K simply follow the Bose statistics [Fig. 4(f)].

The discovery of the collinear AF order with small moment in LaFeAsO [12] has caused much debate about its microscopic origin. Since LaFeAsO is a semimetal, the observed AF order may arise from a SDW instability due to Fermi surface nesting [17–19], where electron itinerancy is important much like incommensurate SDW order in pure metal Cr [20]. Alternatively, there are reasons to believe
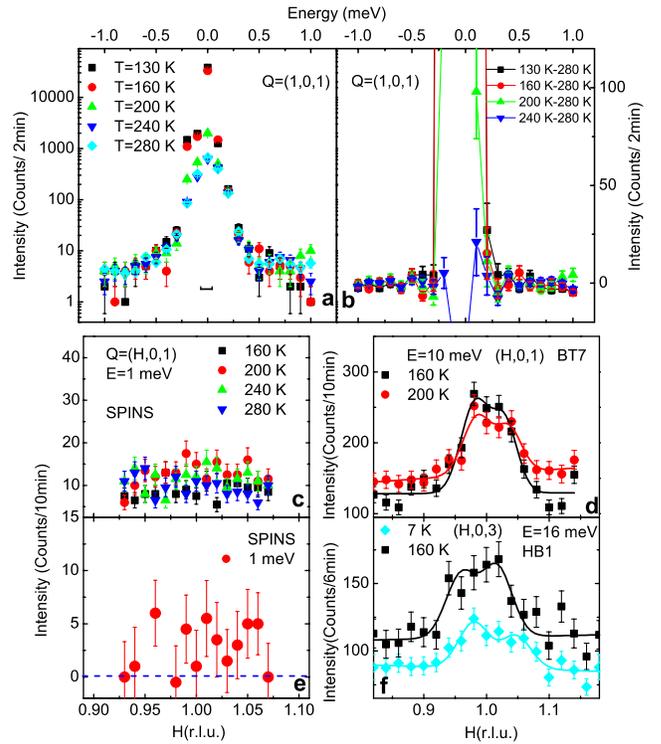


FIG. 4 (color online). Temperature dependence of the quasi-elastic magnetic scattering and spin-wave excitations below and above $T_N$. Data in (a)–(c) are obtained on SPINS. (a) Constant-$Q$ scans at the $Q = (1, 0, 1)$ Bragg peak position at different temperatures. Except for the dramatic increase in the elastic component below $T_N$, the quasielastic scattering above $\hbar\omega = 0.5$ meV is essentially temperature independent, revealing no evidence for the Lorentzian-like paramagnetic scattering above $T_N$ observed in Cr [20]. (b) Temperature difference spectra using $T = 280$ K scattering as background. The data again show little evidence of critical scattering at $\hbar\omega = 1$ meV. (c) $Q$ scans at $\hbar\omega = 1$ meV at different temperatures. We speculate that the slight increase in overall scattering at 240 K from 280 K shown in (e) is due to weakly correlated paramagnetic spins. (d) $\hbar\omega = 10$ meV spin-wave excitations at 160 and 200 K obtained on BT-7. (f) $\hbar\omega = 16$ meV spin-wave excitations at 7 and 160 K obtained on HB-1. The intensity increase is due to the Bose population factor.



FIG. 3 (color online). Temperature dependence of the spin gap obtained from energy scans around the (1,0,1) and (1,0,3) Bragg peaks. (a) Low-temperature ($T = 7$ K) constant-$Q$ scans at the signal [$Q = (1, 0, 1)$] and background [$Q = (1.2, 0, 1)$] positions show a clear spingap of $\Delta = 6.5$ meV. (b) Similar scans at $Q = (1, 0, 3)$ and $Q = (0.8, 0, 3)$ which again show $\Delta = 6.5$ meV. (c), (d) Temperature dependence of the spin gap, where $\Delta = 4.5$ meV at 80 K and $\Delta = 3.5$ meV at 160 K.

that LaFeAsO is in proximity to a Mott insulator [21], and the AF order is a signature of local physics and electron correlations [24,31]. Another heavily debated issue is the first [29] or second [28] order nature of the simultaneous structural or magnetic phase transition in $SrFe_2As_2$.

If the observed AF order in $SrFe_2As_2$ originates from Fermi surface nesting similar to the SDW order in Cr, the velocity of the spin waves $c$ should be $c = \sqrt{v_e v_h / 3}$, where $v_e$ and $v_h$ are the electron and hole Fermi velocities, respectively [20]. The dispersion relation is then $\hbar\omega = cq$ where $q$ is the magnitude of the momentum transfer away from the Bragg position. For Cr, the spin-wave velocity is measured to be $c = 851 \pm 98$ meV Å [20]. In addition, there are strong spin-spin correlations in the paramagnetic state where the dynamic structure factor $S(q, \hbar\omega)$ can be described by the product of a Gaussian centered at the SDW ordering wave vector and a Lorentzian in energy, or $S(q, \hbar\omega) = S_0(T)e^{-\xi/2\sigma^2}(\hbar\omega/k_BT)/[((\hbar\omega)^2 + \Gamma) \times (1 - e^{-\hbar\omega/k_BT})]$, where $\sigma$ and $\Gamma$ are the Gaussian and Lorentzian widths, respectively [20]. At temperatures as high as 500 K ($T = 1.6T_N$), one can observe a clear resolution-broadened Lorentzian centered at $\hbar\omega = 0$ meV with $\Gamma = 15.6$ meV [20]. For comparison, there is no evidence of a Lorentzian-like quasielastic scattering in $SrFe_2As_2$ even at $T = 1.09T_N$. The lack of critical scattering both below and above $T_N$, together with the fact that there is also an abrupt structural distortion occurring at the same temperature and observed thermal hysteresis [15,16,28,29], is consistent with the AF phase transition being first order in nature.

To compare the observed exchange couplings in Fig. 1 and those expected from SDW excitations in a nested Fermi surface, we note that Fermi velocities estimated from the local density approximation calculations for $BaFe_2As_2$ [32] are $v_e = 2.2$ eV Å and $v_h = 1.2$ eV Å. Assuming $BaFe_2As_2$ and $SrFe_2As_2$ have similar Fermi velocities, the expected spin-wave velocity is then $c \sim 0.94$ eV Å. However, since angle resolved photoemission spectroscopy (ARPES) experiments on $BaFe_2As_2$ [33] show that the bandwidth is strongly renormalized, the larger Fermi velocities in electron and hole pockets are $v_e \approx v_h \sim 0.5$ eV Å. These values would give $c \sim 0.29$ eV Å. Using smaller Fermi velocities would yield half of the larger values or $c \sim 0.15$ eV Å. Within the local moment effective $J_{1a} - J_{1b} - J_2$ model, the spin-wave velocity is given by $c = (J_{1a} + 2J_2)a/2$ eV Å. From our measured $J_{1a} + 2J_2 = 100 \pm 20$ meV, $c \sim 0.28$ eV Å which is also fairly close to the ARPES results. Therefore, our present data do not allow an unambiguous distinction between localized and itinerant description of the AF order in $SrFe_2As_2$ in terms of the spin-wave velocity.

In summary, we carried out inelastic neutron scattering experiments to study low energy spin-wave excitations in $SrFe_2As_2$. The low-temperature spectrum consists of a Bragg peak, a spin gap, and sharp spin-wave excitations at higher energies. Using a simple Heisenberg Hamiltonian, we find $J_{1a} + 2J_2 = 100 \pm 20$ meV, $J_z = 5 \pm 1$ meV, and $J_s = 0.015 \pm 0.005$ meV. On warming across $T_N$, there is weak critical scattering and spin-spin correlations in the AF wave vector region explored in the paramagnetic state, different from the paramagnetic SDW excitations in Cr. These results are consistent with the AF phase transition in $SrFe_2As_2$ being first order in nature.

*daip@ornl.gov
[1] P. A. Lee *et al.*, Rev. Mod. Phys. **78**, 17 (2006).
[2] R. Coldea *et al.*, Phys. Rev. Lett. **86**, 5377 (2001).
[3] J. M. Tranquada, in *Handbook of High-Temperature Superconductivity*, edited by J. R. Schrieffer and J. S. Brooks (Springer, New York, 2007), p. 257.
[4] Y. Kamihara *et al.*, J. Am. Chem. Soc. **130**, 3296 (2008).
[5] X. H. Chen *et al.*, Nature (London) **453**, 761 (2008).
[6] G. F. Chen *et al.*, Phys. Rev. Lett. **100**, 247002 (2008).
[7] Zhi-An Ren *et al.*, Europhys. Lett. **83**, 17002 (2008).
[8] M. Rotter *et al.*, Phys. Rev. Lett. **101**, 107006 (2008).
[9] G. F. Chen *et al.*, Chin. Phys. Lett. **25**, 3403 (2008).
[10] K. Sasmal *et al.*, Phys. Rev. Lett. **101**, 107007 (2008).
[11] G. Wu *et al.*, J. Phys. Condens. Matter **20**, 422201 (2008).
[12] C. de la Cruz *et al.*, Nature (London) **453**, 899 (2008).
[13] Y. Chen *et al.*, Phys. Rev. B **78**, 064515 (2008).
[14] Q. Huang *et al.*, arXiv:0806.2776.
[15] Jun Zhao *et al.*, Phys. Rev. B **78**, 140504(R) (2008).
[16] A. I. Goldman *et al.*, Phys. Rev. B **78**, 100506(R) (2008).
[17] J. Dong *et al.*, Europhys. Lett. **83**, 27006 (2008).
[18] I. I. Mazin *et al.*, Phys. Rev. Lett. **101**, 057003 (2008).
[19] I. I. Mazin *et al.*, Phys. Rev. B **78**, 085104 (2008).
[20] E. Fawcett, Rev. Mod. Phys. **60**, 209 (1988).
[21] Q. Si and E. Abrahams, Phys. Rev. Lett. **101**, 076401 (2008).
[22] T. Yildirim, Phys. Rev. Lett. **101**, 057010 (2008).
[23] F. J. Ma, Z. Y. Li, and T. Xiang, arXiv:0804.3370v3.
[24] C. Fang *et al.*, Phys. Rev. B **77**, 224509 (2008).
[25] Z. P. Yin *et al.*, Phys. Rev. Lett. **101**, 047001 (2008).
[26] J.-Q. Yan *et al.*, Phys. Rev. B **78**, 024516 (2008).
[27] G. F. Chen *et al.*, arXiv:0806.2648.
[28] M. Tegel *et al.*, arXiv:0806.4782.
[29] A. Jesche *et al.*, arXiv:0807.0632v1.
[30] D. X. Yao and E. W. Carlson, Phys. Rev. B **78**, 052507 (2008).
[31] C. Xu *et al.*, Phys. Rev. B **78**, 020501 (2008).
[32] F. J. Ma, Z.-Y. Lu, and T. Xiang, arXiv:0806.3526v1.
[33] L. X. Yang *et al.*, arXiv:0806.2627v2.